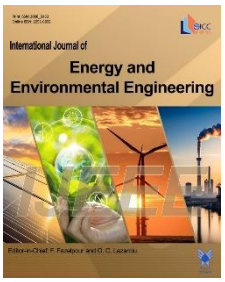

Volume 16, Issue 4, (2025) Article 16

International Journal
of
Energy and Environmental Engineering (IJEEE)

https://doi.org/10.57647/ijeee.2025.1604.16

SARSA: A Novel model for Market Trading Mechanisms and Operational Strategies for Multi-Type Energy Storage Systems in Power Markets

Bin Zhao*，Lining Wang，Bo Wei

China Energy Qinghai Electric Power Co., Ltd., 810001, China

***Corresponding author:** binzhao135@outlook.com

Original Research

Received:
07 July 2025

Accepted:
11 November 2025

Published in Issue:
31 December 2025

Abstract

To maximize performance and profitability, power markets may use a variety of trading methods and operational techniques for multi-type energy storage systems. In accordance with the capacity and structure of the market, these systems may take part in energy markets, supplementary services markets, along with local or P2P marketplaces. With the use of pricing signals and demand estimates, operational strategies aim to maximize income through intelligently charging and releasing the various storage kinds. Regional distribution networks that rely on distribution network operators can now quantitatively determine their energy storage supply and demand with the help of this study's suggested approach for determining Hybrid Golden Flower Pollination (HGFP) Method energy storage action deviations. This method will be crucial for their future participation in market trading. Second, taking into account the economic advantages for all parties involved, the study created a pricing mechanism that incorporates a valley compensation mechanism to encourage autonomous and active user participation using the SARSA Deep Learning technique. The trading mechanism relies on combinatorial auctions and accommodates various types of market participants. Taking into consideration the variations in HGFP energy storage action when different regional networks are involved, numerical simulations were run to confirm the trading mechanism's practicality and rationale.

Keywords: Hybrid Golden Flower Pollination; Market Trading Mechanisms; Multi-Type Energy Storage Systems; Power Market; SARSA Deep Learning technique

Cite this article: Zhao B., Wang L., Wei B., SARSA: A Novel model for Market Trading Mechanisms and Operational Strategies for Multi-Type Energy Storage Systems in Power Markets. Int. J. Energy Environ. Eng. 2025; 16(4) : 1-15. https://doi.org/10.57647/ijeee.2025.1604.16

1. Introduction

Energy storage is an essential tool for distribution networks to reduce power fluctuations caused by renewable energy sources. But energy storage is still an expensive resource, therefore there are a lot of obstacles to its widespread use in power systems [1]. Shared energy storage schemes have recently emerged, opening up new possibilities for the effective management of multi-distribution networks. However, typical centralized scheduling methods have flaws including privacy leakage and excessively cautious decision-making, while operators of distribution networks with shared energy storage systems are separate parties [2]. In the context of energy strategy promotion and electricity market construction, the power grid has the potential to be

economically and environmentally friendly through the large-scale and ongoing integration of renewable energy sources, such as wind and solar power, while flexible resources, such as energy storage [3]. However, it is not without the power system's inherent dangers in terms of safe operation. On the basis of attaining safe functioning of the power grid, it is essential to fully use the synergy of resources and maximize the advantages of different organizations [4]. By taking part in several markets, one may reflect one's position in the power system and make the most of the inherent flexibility of energy storage. The energy and auxiliary service industries have been the primary subjects of previous research on the energy storage industry's involvement in these sectors [5]. Load demand and power pricing in the market have a direct impact on market income. Using energy trading tactics like low-priced charging while high-priced discharging, energy storage may benefit from market price differentials. However, energy storage's high investment cost means that it cannot be adequately incentivized to engage in market operations via the arbitrage of price disparities alone [6]. Energy storage may increase its income streams by entering a joint market rather than just one. An article published in examined the possibility of optimizing energy market arbitrage and fast adjustment ancillary services together, which would greatly increase energy storage's revenue while also taking advantage of its outstanding regulatory performance [7]. In addition, elements such as the capacity industry, reserve market, as well as market participation as shared energy storage are taken into account. Additionally, the reactive power auxiliary services industry has been investigated by a number of academics [8]. To address voltage concerns brought on by dispersed generation's integration into the grid, an incentive structure for the reactive power sector was suggested in. Also, in, researchers looked at how to optimize the scheduling of reactive as well as active power markets simultaneously. Power sales businesses mediate between the wholesale and retail markets for energy, purchasing power from producers in the former and selling it to customers in the latter [9]. The contracts signed by wholesale power sales businesses and the actual energy demand of customers still differ to a certain extent because short-term along with medium-term load forecasts are not always accurate. To keep the system in equilibrium, power sales firms must acquire additional amenities or energy storage facilities to compensate for the errors in electricity load predictions [10]. The reactive power market is still in its infancy in China's power sector. Coordination using active power equipment is a common component of current energy storage operating techniques. This includes working using wind farms or conventional generators. Having said that, the distribution grid is where energy storage is most often seen [11]. Voltage control difficulties are growing in importance as the number of distributed resources increases. It is impossible to ignore the influence of reactive power on the grid's safe and stable functioning [12]. Improving the flexibility and adaptability of electrical systems to accommodate different types of market players is crucial for the growth of new power systems in the paper about the involvement of multiple market members in market-based trading, including wind power, photovoltaics, as well as distributed energy storage. Major obstacles also existed in the process of establishing a contemporary electricity grid. For example, how to increase device utilization, decrease operating costs, and achieve collaborative operation among the regional distribution networks, main grid, and scattered power production and consumption devices; how to improve the grid's operational flexibility; and so on [13].

A. Motivation

Modern power systems are undergoing a transformation due to the integration of multi-type ESSs. These systems include thermal storage, flywheels, pumped hydro, and batteries, all of which improve grid efficiency, dependability, and flexibility. Within the context of competitive energy markets, this research delves into the development and execution of trading mechanisms while operational approaches for these varied ESSs. Taking on technological, financial, and regulatory obstacles is secondary to getting into the energy, capacity, and supplementary services marketplaces. In order to enhance bidding tactics and dispatch procedures, methods driven by optimization, game theory, and machine learning are assessed [14].

B. Contributions

To solve these problems, this research proposes a market method for multi-energy coupling participation based on WT-PV-thermal-ES [15]. Uncertainty around the production of renewable energy sources (RES) and the role of multi-energy coupling in both frequency and energy markets will be further investigated in the suggested system. This study makes the following contributions:

- To deal with the unknowns of WT and PV production, the scenario reduction approach is applied. Examining how RES deal with uncertainty affects market clearing is done using the interval optimization approach.
- A paradigm for cooperative market clearing is put out that incorporates WT, PV, thermal power, along with ES.
- In the combined clearing of frequency and energy regulation auxiliary service markets, this study examines the bidding and revenue circumstances

10.57647/ijeee.2025.1604.16

surrounding multi-energy coupling bodies. Previous research mostly focused on two or three energy outputs that participated in the market.

The following is the outline for the remainder of the paper. In Section 2, we lay out the groundwork for the market and create the RES uncertainty model. Following this, Section 3 introduces the paradigm of WT-PV-thermal-ES involvement in the combined clearing of the frequency and energy regulation auxiliary services segments. Section 4 presents the results of the analysis with the help of examples. Lastly, Section 5 presents the results and recommendations for further research.

2. Related work

No one has looked at the new power system's potential for electrochemical energy storage stations' operational approach [16]. An electrochemical energy storage model that can participate in both the electric energy market and the ancillary service sector is suggested, taking into account the price variations in the electricity market while relying on the conditional value-at-risk model. A typical scenario for electricity prices is first generated from sampling and aggregation via the projection of the power market price. After that, they get the capacity allocation outcomes for various markets based on the suggested operating strategy model. In order to validate the efficacy models, the example analysis is conducted alongside the real-life scenario of the electrochemical energy storage system. Lastly, the impact of various risk choices while market rates on the power station's revenue are examined.

Spot market energy storage using segmented bidding curves is suggested by the authors of [17]. To more accurately represent its scarcity and economic characteristics, energy storage units now bid on energy-price curves rather than power-price curves. A multi-type market joint optimization framework was developed to enable energy storage to take part in the electricity, frequency control, and reserve markets all at once, taking into account the operating features of energy storage. Numerical examples proven the accuracy of the suggested technique.

In [18], the authors provide a method for managing various statistical features of the predicted profit distribution for a wind storage facility using integrated risk monitoring and management. Initially, a framework for risk-averse stochastic decision-making is introduced, along with several risk assessments such as the conditional value at risk, values at risk, and shortfall probability. Next, they provide integrated risk measuring and control methods that take into account the anticipated, boundary, as well as likelihoods of the extreme findings in order to cater to the diverse demands of risk-averse decision makers.

Each of them is handled by CVaR, VaR, and SP, in that order. Lastly, case studies using authentic market data are used to verify the efficiency of the suggested risk management method. The outcomes of alternative risk control techniques are evaluated in detail. Extensive research is conducted into the effects on predicted profits and hazards of various decision-maker risk characteristics, battery storage energy capacity, and day-ahead/real-time pricing differentials.

In order to ensure the secure and reliable functioning of a significant portion of emerging power systems, enhance the effectiveness of energy storage applications, and play a regulatory role, it is necessary to gradually organize the scale while layout of energy storing based on its characteristics and functions, as well as regional energy storage needs (Explorers of [19]). The absence of a thorough benefit assessment is due to the fact that most prior research has concentrated on only one kind of energy storage strategy. From demand analysis and technology selection to capacity planning and energy storage layout, operating mode and full benefit assessment, that article presents a multi-type energy storage planning technique for power systems. As part of capacity planning, they built a model of the power system that accounts for new energy production, and they suggested an optimization approach for the size of multi-type energy storage with the aim of reducing the cost of system energy consumption. The approach of planning was finally shown to be feasible by use of an example.

While the researchers in [20] run their linked units to achieve maximum efficiency, doing so adds complexity and limits flexibility because of the requirement to meet predetermined needs. The potential for low-cost sector coupling within the energy system as a whole may be enhanced by increasing the flexibility of existing as well as future industrial energy systems via energy storage. They provide a design optimization approach that takes into consideration investments in energy storage and the supply of balancing power, with the goal of making industrial energy systems more flexible. Given the unpredictability of the balancing-power request, they provide a stochastic algorithm for the balancing-power market along with suggest two computationally efficient storage models that both yield practical storage operations. A multi-energy system case study found that investing in heat storage and making it easier to participate in the balancing-power market reduced costs by 6–17%. Heat storage is shown to be very beneficial for heat-driven power plants in the sensitivity analysis. To find the best investments that will make the energy system more adaptable to provide balancing power, their strategy takes into account both long-term planning and short-term operating risks.

People that wrote [21] Conventional energy storage methods are costly and time-consuming to build, which

10.57647/ijeee.2025.1604.16

hinders their practicality for widespread use. Researchers are beginning to pay greater attention to demand response, an approach to active management of flexible loads in response to grid demand. That article explores a paradigm for urban load participation in DR dispatch. Electric vehicle load aggregators and building load aggregators combine loads based on type to take part in power grid optimum dispatch, which lowers overall operating cost and requirement for energy storage while decreasing waste from wind and PV. Examples derived from real-world data adjustments confirm the model's validity.

The provincial power system's experts recommend an ideal setup technique for energy storage (see to [22] for details). Its unique selling point is the ability to simulate operations based on the scheduling priorities of different flexible resources, yield the scheduling schemes of those resources in a flash, and then, using metrics like power supply cost, power supply adequacy, and new energy utilization rate, find the optimal configuration capacity of energy storage equipment. The efficiency of the strategy is shown with an example examination of a provincial system that is carried out utilizing the methodology in that article.

That study presented an operational model for optimizing various energy storage systems that takes carbon limits into account, with the goal of addressing the challenge of challenging carbon with electricity coupling as well as novel energy consumption in the evolving electrical grid [23]. An integrated energy system's carbon trading mechanism is built by taking into account the actual carbon emission of a gas turbine. Lastly, a solver is employed to minimize the sum of the carbon trading cost while the operation and maintenance cost. The process begins with the establishment of a mathematical model based on the response characteristics of every energy storage and the corresponding constraints. Following the implementation of the carbon trading mechanism, there was a considerable decrease in carbon emissions, and the findings demonstrate that a more equitable distribution of energy storage proportions improves the economics of system operation.

Improving the system's total energy utilization rate and further optimizing the economics of the new power system was the goal of the experimenters in [24], who suggested using multi-type energy storage collaborative operating technology. The first step was to set up an innovative electrical system design that collaborates with different energy storage. To find the best economic day-ahead scheduling for the new power system, mathematical physics optimization models are run for each subsystem. Finally, that article examines energy storage subsidies through a case study of Xinjiang's actual power system. It compares and verifies the model's effectiveness and superiority under different scenarios, including summer, transition season, while winter, which are typical daily calculation scenarios. Adopting a new power system with partnerships across different types of energy storage decreased the rate of wasteful wind and solar power while optimizing the system's low-carbon and economic performance, according to the findings.

Writers of the cited work [25] It is suggested that a multitype energy storage system be implemented to aid photovoltaic systems in monitoring power scheduling, with a particular focus on VRB grouping state of charge management. That system would include of lithium-ion batteries and vanadium redox flow batteries. Using the permitted deviation ranges of PV's planned power, the power allocation limitations for MESS with the VRB grouping mechanism are first defined. Secondly, an approach to VRB grouping SOC recovery with appropriate charging and discharge thresholds for VRB is developed by considering the effect of VRB on the cycle life of LIB. In the third place, they take into account the cycle life of MESS and the PV power tracking frequency when we build a model for the functioning of the energy storage system and PV. At long last, actual PV data is used to simulate the suggested model. The results prove that the suggested approach is both practical and efficie

3. Proposed work

A. Proposed Market Trading Model

Figure 1 displays the market model that is presented in this research. Thermal power units, energy storage, WT units, and PV units are all energy entities that are part of the market. These energy companies take part in the data transmission spot market and send power to the grid. A grid safety check is carried out after the power trading center's market clearing.

B. Uncertainty Modeling

(i). RES Generation

The fundamental intermittency of wind speed is the primary cause of the uncertainty in the WT output. According to earlier studies, wind speed is distributed according to a Weibull distribution, which is distribution may be expressed mathematically as follows:

$$f(v) = 1 - e^{1-\left(\frac{v}{W_c}\right)^{W_k}}, \quad (1)$$

where W_c stands for the scale parameter, which reflects the wind farm's average speed. It stands for the shape parameter, W_k. where v is the wind speed in meters per second.

The correlation between predicted electricity production and wind speed $P_t^{p-\mu r}$ for WT is as follows:

10.57647/ijeee.2025.1604.16

$$P_t^{verr} = \begin{cases} 0, v \le v_w \\ P_r \frac{v - v_{bs}}{v_r - v_n}, v_{ns} \le v \le v_r \\ P_{rv}, v_r \le v \le v_{avt} \\ 0, v \ge v_{avt} \end{cases} \quad (2)$$

where P_r is the turbine's rated output power. P_t^{www} denotes the anticipated power output of the turbine. v_m stands for the wind speed that was reduced in. v_{oat} measures the wind speed through the cutout.

Solar irradiation and panel configuration parameters are the primary determinants of PV output. The following is a formula for determining the PV system's real electrical power production, supposing that the solar radiation is known:

$$P_t^{prove} = CF \frac{G}{G} P_{protout} \quad (3)$$
$$CF = M_2 \eta_2 \eta_2$$

where P_1^{P-Prr} stands for the anticipated electrical output generated by solar power. G_2 stands for the strength of the sun's rays (W/m^2). G means the usual amount of sunshine, which is set at $1000\ W/m^2$. η stands for the PV modules' conversion efficiency. The PV modules' installation azimuth is represented by η_1. η_2 indicates the efficacy of the PV inverter. η_m stands for the factor that corrects the PV line.

(ii). Load Uncertainty Modeling

The interval (1) may be used to narrow down the range of customer load Q(t) at time t:

$$Q^d(t) \le Q(t) \le Q^r(t) \quad (4)$$

The absolute prediction error of the load is limited in this study using the 1-norm, and the uncertainty coefficient is denoted by the parameter Γ:

$$\frac{\sum_{t=1}^{24} |Q(t) - Q'(t)|}{Q'(t)} \le r_1 \quad (5)$$

wherein Γ_1 Q^' (t) and Q^'' (t) represent the user's highest and minimum loads at time t, respectively, and is the weighted average absolute load error in statistics. The actual load prediction for customers is represented by $Q'(t)$.

(iii). Electricity Price Uncertainty Modeling

The article uses the market price one day from now, at time t, as p(t) t; $p^v p(t)$ is the market price with one day to go at the current moment t; and p^{durn} (t) refers to the lowest price that the market would bare the day after when t :

$$p'^{twn}(t) \le p(t) \le p^{wp}(t)$$
$$\frac{\sum_{t=1}^{24} |p(t) - p'(t)|}{p(t)} \le r_2 \quad (6)$$

wherein Γ_2 is the real price for electricity forecasts, and p^' (t) is the weighted average absolute price mistake in statistics.

Let N be a collection of randomly chosen variables for ζ_1 to ζ_N where M is the value for the sample size. This work uses Latin hypercube sampling as its sampling technique. In this method, the midpoint of each variable's probable range is selected as the sample value, and the m-sample value taken from ζ_N is

$$\xi = F_n^1\left(\frac{m-0.5}{M}\right), n = 1,2,\dots N \quad (7)$$

In systems with several variables, the accuracy of the sample findings may be compromised since the sample matrix produced by the previously described approach does not take into account the inter-correlations between the random variables. Consequently, in order to acquire the set of scenarios, this work use Cholesky decomposition to enhance the order of the sample matrix's components.

For every period's made situation $P_1^{U/J}$, Due to the typical distribution of the produced scenarios, it is possible that some of them may violate the requirements for power production, for example, producing scenarios having a power output below zero. (1) Start by establishing the end goal scenario count, N_i. With an equal chance for each of the first possibilities N_i',

$$H_i' = \frac{1}{N_i'}, i = 1,2,\dots,N_i' \quad (8)$$

Make note of the numbers for the reduction and retention scenarios; select J_1 as the starting reduction scenario and R_6 as the initial retained scenario. (2) Determine how far apart any two possible outcomes are P_u^{1HS} and P_{ij}^{1HS} in R_1, where $i, j = 1,2,\dots,N_i$; Here is the formula for the calculation:

$$e_t^U = \left|P_u^{US} - P_{tu}^{UNS}\right| \quad (9)$$

(3) For any state P_{ij}^{us}, there will be a setting $\min_{4,4f_i^H}^{H}$ Using the following formula, determine the probability product with respect to the shortest path to it:

$$z_i' = r_i' \min_{i,f_i} H_i' = 1,2,\dots,N_i' \quad (10)$$

(4) Between the situations N_i', find the smallest $'_2$, together with the following scenario number:

$$r = \arg \min_{u,-1,2} v_i z_1^2 \quad (11)$$

(5) Revise the collection of proposed reductions $J_i = J_i \cup J^*$ together with the kept scenario group $R_q = R_r \setminus V^*$. (6) Find out whether the value in set R_i has surpassed the predetermined value N_i'. If yes, then stop reducing and make a note of the best possible representative cases; otherwise, go on to step (2).

10.57647/ijeee.2025.1604.16

C. Objective function

Each distribution network's renewable energy production is a combination of centralized wind and solar electricity, with some networks also having distributed energy storage devices, which is given in Fig 1. An objective function to minimize energy expenditures is established by the distribution system operator during operations as well as planning of the network. This function is represented as follows:

$$\min C_t = \min \sum_{t=1}^{T} \left(P_{t,b}^{grid} \lambda_{t,b}^{grid} \Delta t - P_{t,b}^{grid} \lambda_{t,b}^{grid} \Delta t \right) \quad (12)$$

where $P_{t,b}^{grid}$ and $P_{t,s}^{grid}$ express the distribution network's buying and selling power at time t, respectively: $\lambda_{t,b}^{grid}$ besides $\lambda_{t,s}^{grid}$ which stand for the distribution network's buying and selling power prices at time t, respectively. 3.2 Limitations on the electric power balance

$$P_t^{PV} + P_t^{WT} + P_t^{ESd} + P_{t,b}^{grid} = P_t^{load} + P_t^{ESc} + P_{t,s}^{grid} \quad (13)$$

where P_t^{PV} and P_t^{WT} symbolize the distribution network's output from the wind and solar turbines at time t, respectively:

P_t^{ESe} and P_t^{ESd} indicate the power that the distributed energy storage system was able to discharge and charge inside the distribution system at time t, respectively:

P_t^{load} signifies the weight at the current instant in time.

The distributed photovoltaic unit's output model and restrictions are as follows:

$$P_{t,max}^{PV} = \xi_t P^{PV} \quad (14)$$

$$0 \le P_t^{PV} \le P_{t,max}^{PV} \quad (15)$$

where $P_{t,max}^{PV}$ stands for the peak power production of the PV module in the grid at a certain instant t; ξ_t stands for the photovoltaic unit's power ratio at time t, which is affected by variables including solar radiation intensity, light angle of incidence, and panel efficiency; P^{PV} stands for the photovoltaic unit's power ratio at time t, which is affected by variables including solar radiation intensity, light angle of incidence, and panel efficiency:

$$P_{t,max}^{WT} = \zeta_t P^{WT}$$
$$0 \le P_t^{WT} \le P_{t,max}^{WT} \quad (16)$$

where $P_{t,max}^{WT}$ stands for the distribution network's maximum power production from the wind turbine generating unit at the specified time tζ_t is the power-to-noise ratio of the generator unit of the wind turbine at time t, which is affected by variables including wind speed, rotor sweep area, ambient air density, and turbine efficiency:

P^{WT} standing for the distribution network's current capacity of the generating unit of wind turbines.

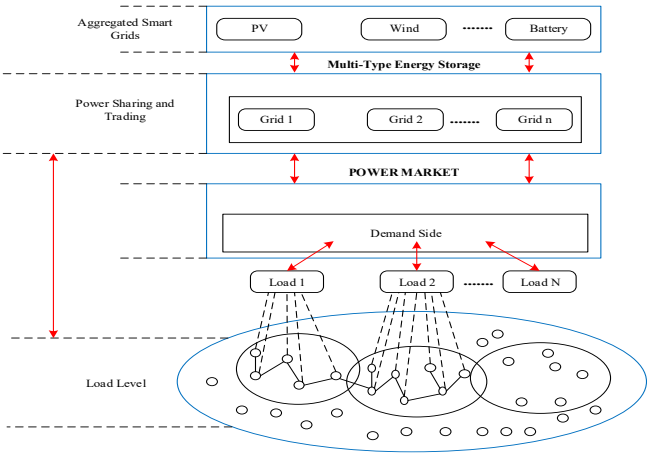

Figure 1. Multi-Type Energy Storage Systems Model

D. Data Windowing

Like many other datasets of its kind, this one uses a small sample size for both its input and output data. The linked data can be of different sizes. In order to solve this, the data has been divided into overlapping windows with predetermined sizes across the time axis. One benefit is that the neural network may process more realizations at once, with each realization being of a constant size.

Learning algorithms and, more specifically, neural network calculations often employ data windowing.

"w" stands for the sample-based window size. In this case, o represents the count of samples that overlap. All the samples inside the original signal's range make up the n-th data window.

$$[(w-o)n, (w-o)n + w - 1] \quad (17)$$

The last step is to combine all the data windows from each subject. The outcome is a data matrix with dimensions $N \times w$. N stands for the overall count of data windows in this case.

E. DKLT

It was expected that using spectral representations of input and output data would be a key part of the suggested technique. This has been accomplished by means of the discrete Karhunen-Loève transform. Its purpose is to decouple the data's fixed properties from its time-dependent components. PCA truncation to principal components of the acquired features is also an option, and a good one. This allows for a simplification of the data. It is common practice to remove unwanted artifacts and noise from signals to reveal their most important data. There is no practical information conveyed by these artifacts.

The approach involves applying singular value decomposition on the initial matrix X:

$$X = USV^T \quad (18)$$

10.57647/ijeee.2025.1604.16

A diagonal matrix S contains one-dimensional values, whereas the single vectors U and V are represented by the variables. With that information, we can calculate a novel matrix:

$$X^* = XV \tag{19}$$

Translating X into the base vector V. Once you've narrowed down the singular values and related vectors of V to a manageable quantity, the PCA can take care of the rest. Matrix truncation to the initial p rows and columns, with p<w, comprising the most significant components, is fundamental to SVD. By reducing the size of X^* to less than X, we can accomplish a reduction in complexity and demonstrate that this leads to improved outcomes.

F. PCA Feature Analysis

One linear transformation method for reducing the dimensionality of multivariate information is PC). Ideally, it would minimize data loss while capturing all of the dataset's variation. One-way PCA simplifies data representation is by turning the initial characteristics into principle components that are linearly uncorrelated.

One way to calculate PCA is:

$$\mathrm{X} = \mathrm{USV}' \tag{20}$$

which include the following: the centered observation matrix (X), the scores matrix (U), the diagonal singular value matrix (S), and the loadings matrix (V).

Principal Component Regression

The benefits of both principal component analysis and linear regression are brought together in principal component regression (PCR). When there are fewer observations than predictor variables, it is a potent technique for high-dimensional data analysis. Build a limited number of principle components and use them as variables in a regression model; that's how PCR works.

One way to calculate PCA is:

$$\mathrm{Y} = \mathrm{XB} + \varepsilon \tag{21}$$

given that Y stands for the response variable, X for the observed predictor matrices, B for the regression coefficient matrix, and ε for the vector of residual errors.

This is the answer to the multiple linear regression problem:

$$\hat{B} = (\mathrm{X}'\mathrm{X})^{-1}\mathrm{X}'\mathrm{Y} \tag{22}$$

By doing PCA on X and then running regression on Y with a subset of the resultant components of X, PCR may minimize collinearity in the predictor variables by identifying a group of orthogonal predictors.

$$\mathrm{X} = \mathrm{USV}' + \varepsilon \tag{23}$$

$$\mathrm{U} = \mathrm{XV} \tag{24}$$

The scoring matrix U, the singular value diagonal matrix S, and the loading matrix V are all used in this context. Here is another way to express the multiple linear regression:

$$\mathrm{Y} = \mathrm{UB} + \varepsilon \tag{25}$$

Here is the formula for the regression solution:

$$\hat{B} = (U'U)^{-1}U'Y \tag{26}$$

An improved variant of PCR is partial least squares regression, abbreviated as MLR. It boosts PCR's predictive power by giving more weight to the predictor factors with the strongest relationships to the response. Like PCA, MLR allows one to express the outer relation for X as:

$$\mathrm{X} = \mathrm{USV}' + \varepsilon \tag{27}$$

Similarly, the Y may be expressed:

$$\begin{aligned} \mathrm{Y} &= \mathrm{TSP}' + \varepsilon^* \\ \mathrm{T} &= \mathrm{YP} \end{aligned} \tag{28}$$

If Y scores are represented by matrix T, singular values are represented by diagonal matrix S, and Y loadings are represented by matrix P. Scores on both X and Y reveal the nature of the relationship between the two variables. This relation's model is expressed as:

$$\hat{t}_l = \mathrm{b}_l \mathrm{u}_t \tag{29}$$

The inclusion of linear combinations of the response and predictor variables in MLR is the key distinction between PCR and MLR. This makes the system more resilient to noisy input and improves prediction performance.

G. HGFP Model

(i). Flower Pollination Algorithm

Essentially, it is based on the same mechanisms that allow flowering plants to pollinate one another. It is undeniable that the FPA has contributed to the resolution of optimization issues. In FPA optimization, there are primarily four guidelines:

First Rule: It is well-known that biotic and cross-pollination are components of global pollination. It departs in search of pollinators according to its levy flying operation.

Second Rule: Abiotic and self-pollinating processes are the backbone of local pollination.

Third Rule: the continued existence of an insect's or pollinator's flowers is proportional to its reproductive likelihood. If two flowers have inversely related similarity functions, then their chances of reproducing are poor.

Fourth Rule: Pollination should be moderately skewed toward local pollination and monitored according to the switch possibilities, whether it's global or local.

10.57647/ijeee.2025.1604.16

When the FPA's updating functions are formulated, these four criteria are transformed into precise updating computations. Licking pollinators, like insects, play an important role in the global pollination process by transporting flower pollen. Furthermore, pollen can travel greater distances due to the greater mobility of long-distance insects. Therefore, Equation (30) lays out the mathematical formulation of the first rule:

$$X_I^{T+1} = X_I^T + \gamma L(\lambda)(g^* - X_I^T) \quad (30)$$

where,

$L(\lambda)$ is the levy flight step size, which is correlated with pollination strength,
γ is the scaling factor used to regulate step size,
g^* is the current best solution,
X_I^T is the pollen I or solution vector, $X - I$, at iteration T,
X_I^{T+1} is the pollen I or solution vector, $X - I$, at iteration $T + 1$.

Flying and moving in steps of varying sizes, insects may cover a lot of ground in the FPA. The most effective way to mimic the movement characteristic is via the Levy flight, a moving circumstance. Hence, Equation (31) might be used to represent a Levy distribution with L>0:

$$L \sim \frac{\lambda\Gamma(\lambda)\sin\left(\frac{\pi\lambda}{2}\right)}{\pi}\frac{1}{M^{1+\lambda}}, (M \gg M_0 > 0) \quad (31)$$

Where the common gamma function is represented by the symbol Γ(Λ). Furthermore, for the long process M>0, this distribution function is valid. This is required in principle, although estimates put the value as low as 0.1. Furthermore, it sidesteps the problem of pseudo-random step sizes that plague this distribution function (8). There are a lot of methods for dealing with random integers. After that, you can think about the local pollination in conjunction with Rules 2 and 3 from Section 4.1. By plugging the results into Equation (32), we may get the local pollination rate.

$$X_l^{T+1} = X_l^T + \epsilon(X_I^T - X_K^T) \quad (32)$$

The different blooms of the same plant kinds are represented by X_J^T and X_K^T, respectively, and the scaling factor ϵ is used to adjust the step size. This pseudocode faithfully reproduces flower constancy in a small neighborhood.

Even the same species may employ a comparable population—also a local random walk with a uniform distribution in [0,1]—to pick its members. The FPA enhances the local pollination method by utilizing the GSA. A comprehensive analysis of the GSA data is provided below.

(ii). Golden Search Algorithm

If your goal functions are either very stable or very hard to differentiate, then this is the way to go for computing them. We may determine the ratio of the golden section using Equation (33).

$$C = \frac{-1+\sqrt{5}}{2} \quad (33)$$

The primary goal is to determine the minimum feasible F(X), where X is an element of R, inside the interval [l,u]. Equations (33) and (34) can be used to calculate the points $X_1, X_2 \in [l, u]$ that constitute two borders.

$$X_1 = Cl + (1 - C)u$$
$$X_2 = Cl + Cu \quad (34)$$

Such that the unimodal optimization curve has two boundaries, X_1 and X_2. I and u represent the lower and upper limits, respectively, on the interval points, while C is the golden ratio. Both of these positions serve to assess the objective function, which is denoted as $f(X_1)$ and $f(X_2)$ accordingly. The optimal variations are related to the interval $[l, u]$ if $f(X_1) < f(X_2)$. In all other cases, the best choices are associated with $[X_1, u]$. Iterate through this process until a termination condition is met. Determining the search sections $[X_1, u]$ and $[l, u]$ for each iteration is necessary. A selection technique is then used to determine the subsequent iterations. In the first GSA iteration, the minor point on the interval $[l, u]$ is calculated. The convergence rate is determined throughout multiple cycles. The use of tent chaos mapping in conjunction with the golden-search-based approach therefore improves the convergence progress performance. Also, it's a part of what makes local search results better. A thorough description of the procedure for the proposed method is provided in the section that follows.

(iii). Optimize Power factors using Hybrid Golden Flower Pollination Algorithm

Tent chaotic mapping unites the FPA and GSA in the hybrid method. The golden-section ratio is used to improve the local pollination process in the FPA. You can end up with the worst exploitation/exploration balance if your optimization technique produces stagnation, traps local optima, and premature convergence. An improved global convergence and the avoidance of traps on a local FPA solution are the goals of the GSFA's creation. As shown in Equation (35) and implemented in the proposed technique, the local pollination of the FPA is enhanced. It is possible to think of the scaling factor ϵ as being dependent on the values of X_1 and X_2, instead of being determined at random. Because it is a black-box procedure, the scale factor influences new source generation. The primary objectives are producing solutions that are associated with a particular likelihood and revising the scale factor. When optimizing your choices, the scale factor is where it's at. For the most optimum processing of the FPA's local search, the proposed algorithm incorporates a new scaling factor.

10.57647/ijeee.2025.1604.16

Equation (35) lays out the procedure, which, in the end, produces two intermediate locations.

$$\epsilon^1 = l - \frac{l-u}{c}; \epsilon^2 = u + \frac{l-u}{c} \quad (35)$$

When selecting a scaling factor, the GSA is a useful tool, which is illustrated in Fig 2.

H. SARSA technique

The SARSA technique is a method for solving RL control issues that is on-policy and uses the time-based difference learning technique. Find the most effective action-value function $\boldsymbol{q}^*$ and the optimal strategy π^* given the following five aspects of an RL context: action space A, state space S, instant reward R, attenuation rate γ, and exploration rate ϵ. At period t, the system transitions to a fresh state s_{t+1}. and simultaneously receives an immediate reward r_t, according to the ϵ-greedy approach. In this fresh state, action $\boldsymbol{a_t}$ is chosen from the current state $\boldsymbol{s_t}$. In the state s_{t+1}. the ϵ greedy method chooses an action a_{t+1}. Action a_{t+1} isn't running right now; it is only being used to change the value function. An equation is used for updating the value function

$$Q_{t+1}(s_t, a_t) = Q_t(s_t, a_t) + \alpha\big(r_t + \gamma Q_t(s_{t+1}, a_{t+1}) - Q_t(s_t, a_t)\big) \quad (36)$$

α represents the learning factor, while γ stands for the discount factor. To enhance the method, the SARSA (λ) technique is an alternative to the normal SARSA algorithm. Although SARSA (0) only updates the previous step after each action in SARSA, SARSA (λ) may revise the step before the reward if the trace decay factor λ is in the range of 0 to 1. Λ, which is equivalent to the future value of predicted Q, represents the chance for the agent to revisit the prior path after revising the Q-table following the agent's reward. The agent essentially places a flag on the ground with each step and gradually reduces its size with each step. To calculate λ-return, add up the benefits from each step n from 1 to infinity times the weight. Every step's weight is (1-λ)^(n-1), hence the equation for calculating λ-return is given as

$$G_t^{\lambda} = (1-\lambda)\sum_{n=1}^{\infty} \lambda^{n-1} G_t^{(n)} \quad (37)$$

In contrast to SARSA, its algorithm incorporates an extra matrix $E[s,a]$ (eligibility records) to record the relative importance of each step leading up to the next reward, here described as

$$E_0(s,a) = 0$$
$$E_t(s,a) = \begin{cases} \gamma\lambda E_{t-1}(s,a) \text{ if } (s,a) \neq (s_k, a_k) \\ \gamma\lambda E_{t-1}(s,a) + 1 \text{ if } (s,a) = (s_k, a_k) \end{cases} \quad (38)$$

The best approach can be learned more quickly and more efficiently using SARSA(λ). Some Q-values may suggest that action an is good, while others may suggest that it is bad, because action an in the Q-table can be mapped to multiple states. In order to more accurately assess the action's quality, the first stages are revised only once the reward is determined. Thus, SARSA(Λ) converges more quickly under the correct Λ. In a SARSA, the state or action function is assessed using DQN in relation to the present state and action. A reward is supposed to be provided for every condition and activity. Deep Q-network's sophisticated learning technique maps states and actions using QTable. The learning environment is a place where the agent may observe, act, and receive rewards. In order to anticipate a stroke, the suggested work makes use of the network's prediction function, which determines the optimal course of action to take next. Experience replays while iterative update are two methodologies that are part of DQN's update mechanism. The iterative update technique aims to decrease the relationship among Q-values and the goal, whereas the experience replay uses a data randomization process to smoothen the data and address the correlation issue.

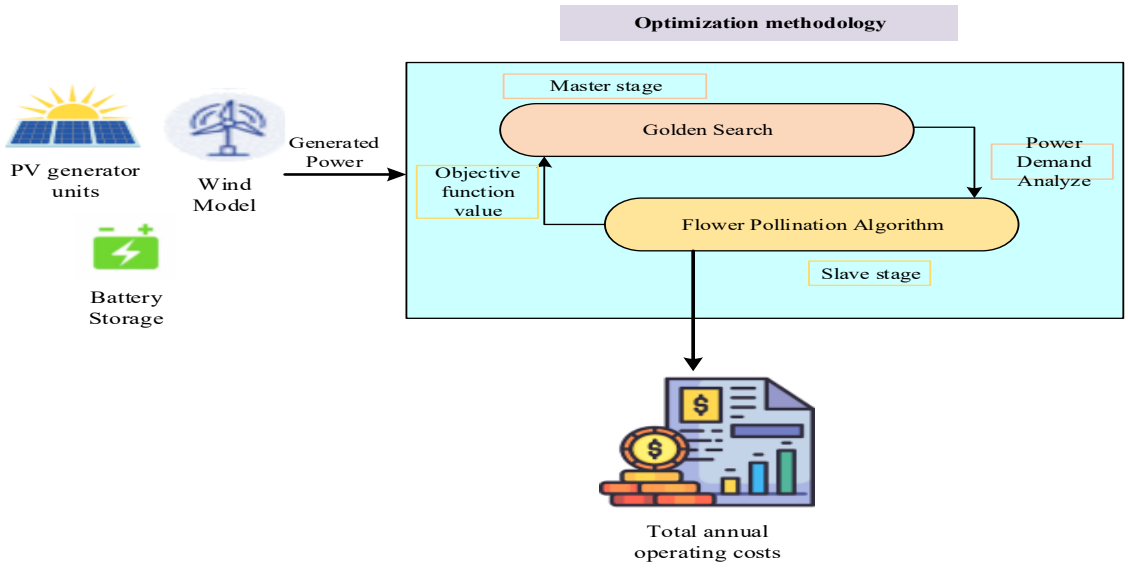

Figure 2. Demand Response and Cost Prediction using Multi-Type Energy Storage Model

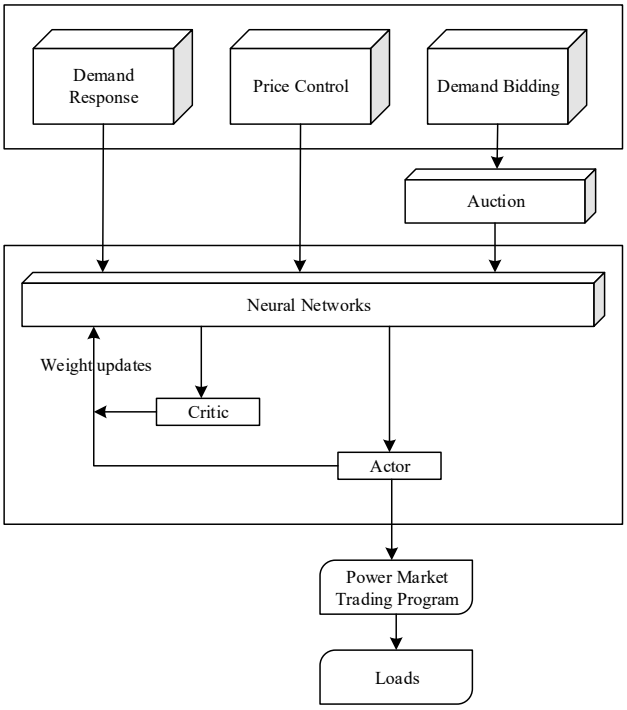

Figure 3. Overall Power Control using SARSA DRL

The following mathematical formulation of the loss function is achieved by using these update tactics; this in turn reduces the mean squared error throughout the prediction phase.

$$l = (r + \gamma_{a'}^{max} Q(s', a'; \theta') - Q(s, a; \theta))^2 \quad (39)$$

where $Q(s, a; \theta)$ where η stands for the discount factor and is the present estimate.

Model Description

For this, we rely on the feature subset that emerged from the K-Nearest Neighbor classifier evaluation. The effect of data imbalance on feature selection was taken into account while designing the objective function, which took the length of the feature subset and the second-order categorization error rate into account, which is given in Fig 3,

$$\text{fitness} = \mu \cdot \text{balanced\_error} + (1 - \mu) \cdot \frac{sf}{nf} \quad (40)$$

where sf denotes the length of the feature subset that was chosen; The data collection contains an infinite number of features, denoted as nf; μ is a component that helps to maintain a stable classification error rate as the feature subset length increases, and

$$\text{balanced\_error} = \frac{1}{n} * \sum_{k=1}^{n} \left(1 - \frac{TP_k}{|S_k|}\right)^2 \quad (41)$$

where n is the count of issues in classes, TP_k is the count of examples in class k that were properly categorized, and S_k is the count of every instance in class k. Classes with few occurrences may be better classified by penalizing underperforming classes with the square of the classification mistake rate.

This is important to keep in mind since the dataset contains classes with a large number of instances and classes with a small number of instances. issue A has only one case while issue B has nine examples in a binary categorization issue with ten instances. Classifying all cases as issue B allows the classifier to quickly attain 90% classification accuracy. While this looks efficient, the technique will not perform well when faced with real-world situations. The computational cost of the approach will be significantly increased, particularly for high-dimensional problems, if the classification error rate is the sole metric considered. This is because the chosen feature subset will include more redundant features. With this goal in mind, we minimize the proportion of the number of features that were picked to all features by making the dimension of the feature subset an objective function.

We train the first model on the completely labeled dataset and then use it for forecasting labels for samples without labels in our framework. To ensure that only very definite predictions are chosen as pseudo labels, a high level of confidence is enforced. By using this selection method, we can reduce the likelihood of adding inaccurate or noisy labels to the training set and increase the likelihood of adding only solid predictions. Since the new data set include both the original labels and the pseudo-labeled models, it offers a more varied and comprehensive collection of training instances.

An f(x) probability distribution across the target classes is generated by the model for every unlabeled sample x. Confidence score for x is defined as:

10.57647/ijeee.2025.1604.16

$$s(x) = \max_c f(x)_c \quad (42)$$

where $f(x)_c$ indicates the projected likelihood for class c. A pseudo label y_p is subsequently given to x if its confidence score reaches or exceeds a predetermined threshold τ (e.g., 0.8):

$$y_p = \begin{cases} \arg\max_c f(x)_c, & \text{if } s(x) \geq \tau, \\ \text{discarded}, & \text{otherwise.} \end{cases} \quad (43)$$

Only samples with $s(x) \geq \tau$ are kept and included in the list of items for training. The model is then fine-tuned using this larger dataset, which improves its generalizability and performance.

G. Design of Trading Mechanism

The majority of the cross-regional energy dispatch continues to occur in advance since China's model for trading across provinces is still in its early stages. After subtracting the initial national export plan, the power systems in the provinces may be roughly modeled as self-balancing regions. Meanwhile, the regional self-balancing mechanism is expected to meet rising demands as a result of China's renewable energy consumption responsibility structure, which places a greater focus on territorial oversight of renewable energy consumption.

Within the framework of China's actuality, the primary objective of this piece is to attain a balance of on-site renewable energy consumption by achieving maximum localized consumption of fresh energy while maintaining profitability. This allows for a more accurate verification of the model's efficacy and the attainment of an optimal matching supply of power within the limitations of pertinent grid operation indicators, as regional self-balancing usage is more severe for provinces using abundant renewable energy contrasted to the scenario of free cross-border energy flow.

Providers of energy storage services can smooth out power system fluctuations, allowing for the seamless execution of Clean Energy Collaborative consumption transactions. An energy storage system may be used to store surplus power when the output of power production surpasses the maximum regulatory level of user demand with demand-side resources. It is also possible to get the power need from the electricity storage system when the generating output value is less than the minimum operational load amount for user demand as well as demand-side resources. The supplier of the distributed energy storage services makes a profit and gets a return on investment from the two groups of people that utilize the equipment.

The primary entity that takes part in the consumption-sharing transaction might also trade in green certificates and excess consumption. Users may earn extra money by selling their surplus renewable energy quota index on the excessive consumption exchange market. In order to generate extra revenue, clean energy power generating firms may participate in the green certificates trading market. This is particularly true for non-water renewable energy power production companies.

Currently, a market-based mechanism determines the price of shared energy storage. Users can bid on the capacity and power of the storage device to gain access to using it continuously for a set period of time. Furthermore, its charging and discharge power can be adjusted with ease to meet user needs. The ultimate pricing is very sensitive to market circumstances since power rights along with capacity rights of energy storage are priced via market-based bidding. This study suggests a technique for calculating the price of power rights as well as capacity right, as stated in formula (44), using the studies in the literature mentioned above:

$$Q'_{SS_n} = \frac{V'_{SS_n} * res^{t-1}_{SS_n}}{P'_{SS_n}} \times Q\left(T'_{SS_n}\right) \quad (44)$$

where $RANK'_{SS_n}$ in the j-th quote, the dispatching sequence of provider i, a shared energy storage service, and V'_{SS_n} is its adjustment capacity; $res^{t-1}_{SS_n}$ is the level of historical reaction, with a value in, produced from the complete score of the energy storage quotient's level of performance at the historical level [0,1]; P'_{SS_n} is its service price; $\text{RANK}\left(T^J_{S_n}\right)$ according to the moment of declaration. "×" denotes a calculating logic that goes like this: before clearing, determine the applicant's capacity, price, along with historical response level proportion to get a full picture of its economic and practical indicators. These indications work according to the following logic: When both the price and adjustment capacity are kept constant, a lower price results in a higher comprehensive index coefficient and a higher ranking; conversely, when both the price and adjustment ability are kept constant, a higher comprehensive index coefficient and a higher ranking are achieved. We will rank the two declaration organizations due to their declaration duration, with the earlier the time, the better the rating, if their comprehensive indications are equal.

Both the pre-use maintaining capacity of the shared energy storage facility in the collaborative consumption trading technique and the safety margin are components of the maximum regulating demand capacity for the following day. The former is derived from the imbalance between the power generation side while the power side, while the latter is based on the work experience of the power dispatching personnel and can rise to a certain percentage using the pre-use adjustment capacity derived from past data. One kind of ANN is a multilayer perceptron. For a variety of purposes, it finds widespread use in deep learning and machine learning. Activities such as pattern recognition, categorization, and regression fall under this category. In the realm of neural networks, it is

10.57647/ijeee.2025.1604.16

an essential design. The building blocks of a MLP are linked nodes, or neurons, arranged hierarchically:

- Input Layer: This layer gets the raw info that came in. The input layer is where the neurons are mapped to specific features of the data that is being input.
- Hidden Layers: All the way between the input and output layers are one or more additional layers. In a hidden layer, every neuron receives data from its predecessors. The inputs are combined linearly. After that, a non-linear activation function is applied. The goal for all of these hidden layers is to discover intricate data patterns and connections.
- Output Layer: This layer is responsible for creating the network's result. The task at hand determines the optimal number of neurons for the output layer.

The design and neural network utilized in this work are an MLP. There are three dense layers that make it up. The input data's dimensions are matched by the first layer. The output data's dimensions are matched by the final layer. They are connected by an extra secret layer. The input data has a dimension of $N\times50$. In this case, Q represents the predetermined dimension of the data batch by the network. The quantity of components kept in the PCA is 50. Overfitting is an issue that can arise during the neural network's training process. When a network's variables are overfit to the training data, it's considered overfitting. Because of this, the model performs poorly when tested and validated using data that the network has never seen before. There are a lot of ways to lessen the impact of this issue. The use of dropout layers is a straightforward and efficient technique. Each of these layers randomly discards some data at various points along the processing chain. This keeps the network from being overfit with the same data at each stage.

Loss Function

Loss functions are used to help the neural network be optimized on a global level. During training, the loss function pushes the network in the direction of its ideal value for parameters. In most cases, the network's intended use case dictates the loss function to be used. For instance, the sparse categorical cross-entropy function is a good loss function for a network that is classifying things into more than one group. MSE and other general loss functions can be helpful in broader applications, such as non-linear function regression. Here, finding the input-output components that are most correlated is the goal of the job. As a result, we have built a bespoke loss function. This loss function's goal is to reduce the discrepancy between the expected and actual data's input-output correlation. To be more precise, the loss function is

$$J(W) = |\rho(x,\hat{y}) - \rho(x,y)| \tag{45}$$

W stands for the collection of parameters used by the network, whereas x represents the input used by the network. The anticipated output is represented by $\hat{y}$, while the true output is denoted by y. The coefficient of Pearson correlation is represented by $\rho(\cdot,\cdot)$.

4. Results and discussion

A. Experiments

This research set up four distribution networks, each with its own set of wind turbines, solar panels, and scattered energy storage devices, to run simulations and see whether the suggested trading mechanism worked. Each distribution network's day-ahead wind and solar power output projections with original load curves are given, along with the intraday actual power production and load curves, which is given in equation 4.

B. Case Study

Here, we use the IEEE 33-bus distribution network to check whether the strategy is effective. The suggested method's testing network structure is shown in Fig. 4. Every node's active power along with reactive power load are allocated proportionately according to the observed curve. One of them, node 1, is linked to the upper market, while each of the distribution network's nodes (G1–G4) is connected to a typical generator. Table 1 contains the settings of the controlled devices. Table 2 contains the parameters of the two energy storages that are allotted to the distribution network, S1 and S2. Table 1 and 2 lists the main parameters utilized to create the models, whereas Table 3 highlights the requirements of the development environment.

C. Multi-Type Energy Storage Efficiency Analysis

A Multi-Type Energy Storage Efficiency performance measure and a confusion matrix were used to test market trading mechanisms. A total of four important factors formed the basis for the classification metrics for performance.

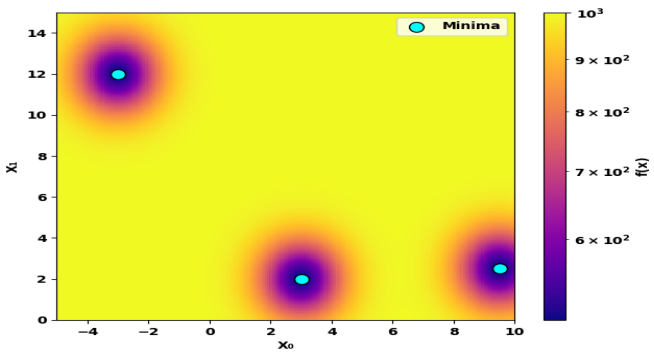

Figure 4. Trading Locations Spotting

10.57647/ijeee.2025.1604.16

The true-positive (TP), false-negative (TN), and true-negative (FN) values are these indications. What we call "true positives" is the percentage of positive samples that were actually identified. The amount of samples that were mistakenly labeled as positive is called false positives. How many samples were accurately predicted to be negative is called the "true negative" count. The amount of positive samples that are wrongly projected as negative is called false negatives.The classification performance metrics included classification accuracy (*Acc*), *precision*, *recall*, and *F*1 *score*.

Classification accuracy is the ratio of correctly predicted samples to the total number of samples, with higher *Acc* indicating stronger overall model performance; *precision* is the proportion of true positives among all positive predictions, with higher *precision* indicating lower error rates when dealing with positive samples; *recall* is the proportion of true positives among all actual positives, with higher *recall* indicating the better ability of the model to correctly identify the category; *F*1 *score* is the harmonic mean of *recall* and *precision*, with a higher *F*1 *score* indicating a better balance between coverage and recognition ability, leading to higher performance on datasets with different class sample sizes. The calculation of classification performance metrics is given by Equations (46)–(49).

$$Acc = \frac{TP+TN}{TP++TN+FP+FN} \tag{46}$$

$$\text{Precision} = \frac{TP}{TP+FP}, \tag{47}$$

$$\text{Recall} = \frac{TP}{TP+FN} \tag{48}$$

$$\text{F1 Score} = \frac{2\cdot(\text{Precision}\cdot\text{Recall})}{\text{Precision}+\text{Recall}} \tag{49}$$

Some of the success metrics for classification were accuracy, precision, recall, and F1 score. The percentage of samples that were accurately predicted relative to the overall number of samples is known as classification accuracy. The general efficacy of the model is strengthened by greater precision (Acc).

Accuracy can be defined as the ratio of correct forecasts to total positive predictions. There will be fewer mistakes when working with positive samples if the accuracy is high. As a percentage of all good results, recall measures how many were actually accurate. A higher recall number shows that the model is doing a better job of identifying the category. When recall and precision are harmonically averaged, the result is the F1 score. An improved coverage-to-recognition ratio is shown by a higher F1 score.

This improves performance on datasets where the number of classes varies. Equations (48)–(49) provide the formulas for calculating classification evaluation metrics.

Table 1. Adjusting the parameters of the generator unit

Parameters	Proportion	Price (USD/MW)	Position of the Node Number	Pmax (MW)
G1	9	47.67	17	40
G2	22	43.99	26	30
G3	14	47.06	29	90
G4	12	59	6	70

Table 2. Configuration of energy storage parameters

Parameters	SOCmax/SOCmin	$\eta ck/\eta dk$	Position of the Node Number	Max Cap (MW·h)	Pmax (MW)
S1	0.8/0.2	0.95/0.96	19	80	30
S2	0.9/0.3	0.95/0.96	29	30	20

Table 3. Specifications of development environment

Specification	Value
Processor	TPU
RAM	35.35 GB
Disk Space	2 T
Data Storage space	Google Drive
Development platform	Python 3.6

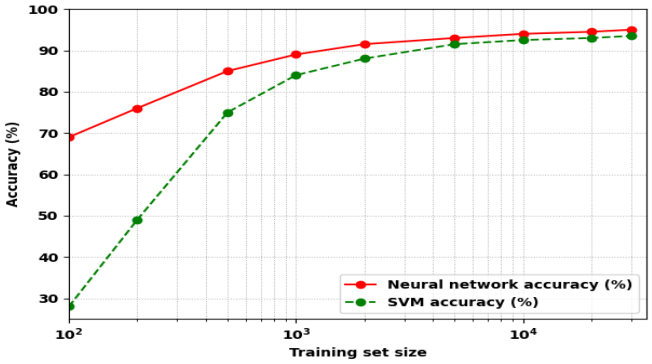

Figure 5. Comparison of Accuracy

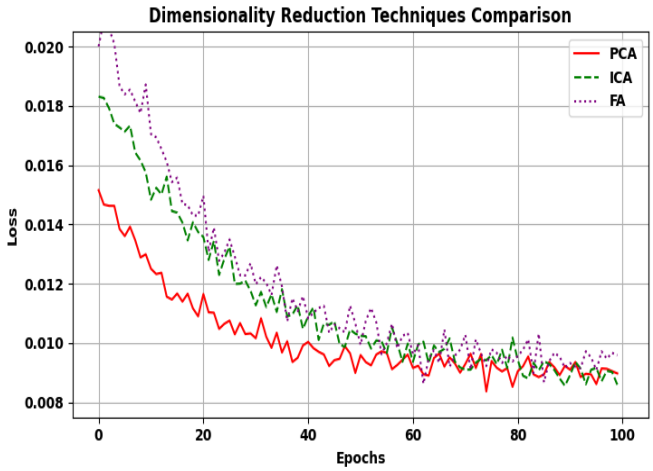

Figure 6. Loss for PCA Model

10.57647/ijeee.2025.1604.16

When looking at accuracy, a greater value indicates that the model is better at classifying data generally, meaning it can identify the majority of samples with more precision. In terms of accuracy, a greater value indicates that the model's positive sample predictions are more likely to be correct. In terms of recall, a higher number indicates that the model is better able to detect and locate TP values. In terms of the F1 score, a greater value indicates that the model strikes a positive balance among recall and precision. This proves first-rate results on datasets where class-specific sample numbers vary, which is given in Fig 5 and Fig 6.

One of the most useful supervised learning tools for DL is a confusion matrix. The output is a synopsis of the predictions made by a classification model. The recognition performance of the model can be seen visually. A matrix format is used to display the data. Record sets in the dataset are organized using the matrix based on the real and expected categories. Fig. 6 shows the daily load fluctuations before and after demand response was implemented. This results in a reduced peak-valley load differential, which in turn reduces the strain on renewable energy production and the energy storage system, as the load is moved from peak to valley hours of power prices. The outcome is a decrease in the microgrid units' configured capacity. To sum up, it's clear that demand response lessens the power disparity among supply and demand and eases strain on the energy storage system. This, in turn, lowers the configured capacity for SVM and Neural networks, which leads to a small drop in microgrid supply dependability. The total profit has improved despite the decline in the system's operational income due to the higher investment and O&M expenditures.

5. Conclusion

Improving network versatility and effectiveness, multi-type energy storage systems provide multiple operating methods and trading mechanisms inside power markets. Various market sectors, such as energy arbitrage, supplementary services, and local flexibility markets, are served by these systems, which include pumped hydro, batteries, and compressed air. Complex models and trading tactics taking storage properties, market dynamics, and renewable energy source integration into account are necessary for optimal functioning. Important factors influencing energy trading include changes in environmental competition, market power pricing, socioeconomic status, and load. In addition to electrical and thermal energies, other types of energy, such hydrogen, may be stored in multi-type energy storage systems. Future study will thoroughly examine these elements in order to design energy trading techniques that are more stable.

10.57647/ijeee.2025.1604.16

Ethics approval and consent to participate
I confirm that all the research meets ethical guidelines and adheres to the legal requirements of the study country.

Consent for publication
I confirm that any participants (or their guardians if unable to give informed consent, or next of kin, if deceased) who may be identifiable through the manuscript (such as a case report), have been given an opportunity to review the final manuscript and have provided written consent to publish.

Availability of data and materials
The data used to support the findings of this study are available from the corresponding author upon request.

Competing interests: here are no have no conflicts of interest to declare.

Authors' contributions (Individual contribution): All authors contributed to the study conception and design. All authors read and approved the final manuscript

References

1. Yu, J., Du, F., Fan, F., Zhang, X., Chen, X., & Qin, Y. (2024). Resource Allocation Method for Grid-Side Hybrid Energy Storage Considering Bidding and Operation Strategies. 2024 IEEE 8th Conference on Energy Internet and Energy System Integration (EI2), 2189-2194.
2. Lago, J., Suryanarayana, G., Sogancioglu, E., & de Schutter, B. (2021). Optimal Control Strategies for Seasonal Thermal Energy Storage Systems With Market Interaction. IEEE Transactions on Control Systems Technology, 29, 1891-1906.
3. Song, W., Jin, Q., Zhang, K., Zhu, Q., Kang, K., & Jia, H. (2025). Decision-Making in Energy Storage Participation in Multi-Variety Power Market Transactions. 2025 10th Asia Conference on Power and Electrical Engineering (ACPEE), 1827-1835.
4. Xiang, Z., Huang, C., & Li, K. (2023). Strategic Bidding of Load Aggregator in Demand Response Market Considering Shared Energy Storage. 2023 IEEE/IAS Industrial and Commercial Power System Asia (I&CPS Asia), 2273-2280.
5. dos Santos, A.F., & Saraiva, J.T. (2023). Decentralized and Centralized Storage Architectures in Local Energy Markets (LEM) and Their Interaction with the Wholesale Market (WSM). 2023 IEEE Belgrade PowerTech, 1-6.
6. Huang, F., Fan, H., Shang, Y., Wei, Y., Almutairi, S.Z., Alharbi, A.M., Ma, H., & Wang, H. (2024). Research on Renewable Energy Trading Strategies Based on Evolutionary Game Theory. Sustainability.
7. Alabdullatif, A.M., Gerding, E.H., & Perez-Diaz, A. (2020). Market Design and Trading Strategies for Community Energy Markets with Storage and Renewable Supply. Energies.
8. Yang, P., Li, X., Yang, C., & Chen, L. (2025). A Dynamic Pricing Model Incorporating Renewable Energy Station Out-put Forecast Deviation and Shared Energy Storage State of Charge. 2025 10th Asia Conference on Power and Electrical Engineering (ACPEE), 2399-2404.
9. Tadayon, L., & Frey, G. (2025). Multi-Level Simulation Framework for Degradation-Aware Operation of a Large-Scale Battery Energy Storage Systems. Energies.

10. Rajah, I., Sowe, J., Schimpe, M., & Barreras, J.V. (2024). Degradation-Aware Derating of Lithium-Ion Battery Energy Storage Systems in the UK Power Market. Electronics.

11. Hu, D., Bian, H., Wang, X., Zhang, Z., & Ma, L. (2024). Research on quotation strategy and clearing model of energy storage participating in power market. 2024 IEEE 4th International Conference on Information Technology, Big Data and Artificial Intelligence (ICIBA), 4, 26-30.

12. Lu, K., Hong, C., Lian, J., & Cheng, F. (2025). A Review of Synergies Between Advanced Grid Integration Strategies and Carbon Market for Wind Energy Development. Energies.

13. Jia, K., Zhang, S., Islam, M.M., Yu, T., Ying, W., & Zhao, Y. (2024). Optimization of Multi-Microgrid Energy Trading in Distribution Networks Using a Master-Slave Game Approach. 2024 IEEE International Humanitarian Technologies Conference (IHTC), 1-6.

14. Yao, H., Hakimian, V., Farrokhabadi, M., & Zareipour, H. (2025). Emission-Aware Operation of Electrical Energy Storage Systems. ArXiv, abs/2506.16454.

15. Yang, K., Yu, Q., Wu, J., & Lin, W. (2025). Research on Optimal Scheduling of Multi-micro-grid-Shared Energy Storage Power Station Based on Improved Vulture Algorithm. 2025 8th International Conference on Energy, Electrical and Power Engineering (CEEPE), 1308-1313.

16. Yang, K., Sun, Q., Fan, H., Li, J., Wang, Y., & Zhang, W. (2022). Joint Operation Strategy of Electrochemical Energy Storage Station Participating in Multi-type Electricity Markets. 2022 IEEE Transportation Electrification Conference and Expo, Asia-Pacific (ITEC Asia-Pacific), 1-6.

17. Yang, D., Wei, Y., Li, M., Xu, G., & Zhao, L. (2023). A Multi-type Market Joint Optimization Model Considering Energy Storage Participation. 2023 5th International Conference on Power and Energy Technology (ICPET), 1693-1698.

18. Xiao, D., Chen, H., Cai, W., Wei, C., & Zhao, Z. (2023). Integrated risk measurement and control for stochastic energy trading of a wind storage system in electricity markets. Protection and Control of Modern Power Systems, 8, 1-11.

19. Wei, B., Qiao, W., Teng, M., Zhang, Y., He, P., Yang, J., Li, J., & Yanan, Z. (2024). Multi-type Energy Storage Planning Method for A High Proportion of New Energy Power Systems. 2024 4th Power System and Green Energy Conference (PSGEC), 586-592.

20. Nolzen, N., Leenders, L., & Bardow, A. (2023). Flexibility-expansion planning of multi-energy systems by energy storage for participating in balancing-power markets. Frontiers in Energy Research.

21. Bai, J., Ding, T., Feng, S., Sun, Y., Zhu, J., & Su, F. (2023). Demand Response by Urban Multi-type Load Aggregators and Storage Systems in Power Grid. 2023 International Conference on Future Energy Solutions (FES), 1-6.

22. Hu, J., Meng, Z., Huang, B., Li, N., Shi, Z., & Sun, B. (2023). Optimal configuration method of energy storage in provincial power system based on multi-type flexible resource scheduling priority. 2023 3rd International Conference on Intelligent Power and Systems (ICIPS), 703-706.

23. Zhou, T., Zhanga, C., Liu, Z., Wang, S., Zhao, Z., & Tang, F. (2024). Optimization strategy of multi-type energy storage considering carbon constraints. 2024 6th International Conference on Energy, Power and Grid (ICEPG), 312-317.

24. Yang, G., Zhu, Y., Lai, R., Li, J., Chen, H., & Pan, P. (2023). Modelling of Optimal scheduling scheme for a power system operation with multi-energy storage systems. 2023 6th International Conference on Renewable Energy and Power Engineering (REPE), 276-282.

25. Chu, Y., Yang, H., Ma, Y., Sun, L., Yang, Z., & Xie, X. (2023). Multi-type Energy Storage System Operation Strategy Based on Grouping State of Charge Regulation. 2023 IEEE 7th Conference on Energy Internet and Energy System Integration (EI2), 4692-4697.